Supporting Information for

Anisotropic Nodal Loop in NiB_2 Monolayer with Nonsymmorphic Configuration

Qian Xia,[†a] Yang Hu,[† a] Ya-ping Wang,[b] Chang-wen Zhang,[a] Miao-juan Ren,[a] Sheng-shi Li[*a] and Wei-xiao Ji[*a]

[a] *Spintronics Institute, School of Physics and Technology, University of Jinan, Jinan, Shandong 250022, P. R. China*

[b] *State Key Laboratory of Crystal Materials and Institute of Crystal Materials, Shandong University, Jinan, Shandong 250100, P. R. China*

† *These authors contributed equally to this work.*

* *Corresponding authors*

Table S1 Calculated Fermi velocity (v_F) and effective mass of electron (m_e*) at different band crossings for free standing and stressed NiB_2 monolayer.

Type of strains	coefficient of strain		P_1	P_2	P_3
None	0%	v_F (m/s)	5.56×10^{5} m/s	1.16×10^{6} m/s	6.90×10^{5} m/s
		$\lvert m_e^* \rvert$	4.70×10^{-5} m_0	2.50×10^{-5} m_0	2.85×10^{-5} m_0
Uniaxial strain along a direction	4%	v_F (m/s)	7.38×10^{5} m/s	1.13×10^{6} m/s	8.19×10^{5} m/s
		$\lvert m_e^* \rvert$	3.51×10^{-5} m_0	2.58×10^{-5} m_0	2.30×10^{-5} m_0
	6%	v_F (m/s)	7.36×10^{5} m/s	6.68×10^{5} m/s	7.78×10^{5} m/s
		$\lvert m_e^* \rvert$	3.51×10^{-5} m_0	4.37×10^{-5} m_0	2.38×10^{-5} m_0
Uniaxial strain along b direction	4%	v_F (m/s)	7.83×10^{5} m/s	1.14×10^{6} m/s	7.16×10^{5} m/s
		$\lvert m_e^* \rvert$	3.24×10^{-5} m_0	2.47×10^{-5} m_0	2.74×10^{-5} m_0
	6%	v_F (m/s)	7.91×10^{5} m/s	1.12×10^{6} m/s	7.11×10^{5} m/s
		$\lvert m_e^* \rvert$	3.16×10^{-5} m_0	2.46×10^{-5} m_0	2.76×10^{-5} m_0
Biaxial strain	4%	v_F (m/s)	5.64×10^{5} m/s	1.19×10^{6} m/s	7.83×10^{5} m/s
		$\lvert m_e^* \rvert$	4.46×10^{-5} m_0	2.36×10^{-5} m_0	2.41×10^{-5} m_0
	6%	v_F (m/s)	7.48×10^{5} m/s	1.19×10^{6} m/s	8.18×10^{5} m/s
		$\lvert m_e^* \rvert$	3.30×10^{-5} m_0	2.32×10^{-5} m_0	2.27×10^{-5} m_0

Table S2 Calculated magnetic ground state of MB_2 (M=Sc, Ti, V, Cr, Mn, Fe, Co, Cu, Zn) monolayers.

Structures	Magnetic ground state	Notes
ScB_2	Nonmagnetic state	/
TiB_2	Nonmagnetic state	/
VB_2	Ferromagnetic state	E(FM) – E(AFM) = –0.30eV
		E(FM) – E(NM) = –0.89eV
CrB_2	Ferromagnetic state	E(FM) – E(AFM) = –1.48eV
		E(FM) – E(NM) = –3.20eV
MnB_2	Antiferromagnetic state	E(AFM) – E(FM) = –0.20eV
		E(AFM) – E(NM) = –5.07eV
FeB_2	Antiferromagnetic state	E(AFM) – E(FM) = –0.22eV
		E(AFM) – E(NM) = –3.95eV
CoB_2	Ferromagnetic state	E(FM) – E(AFM) = –0.05eV
		E(FM) – E(NM) = –1.90eV
CuB_2	Nonmagnetic state	/
ZnB_2	Nonmagnetic state	/

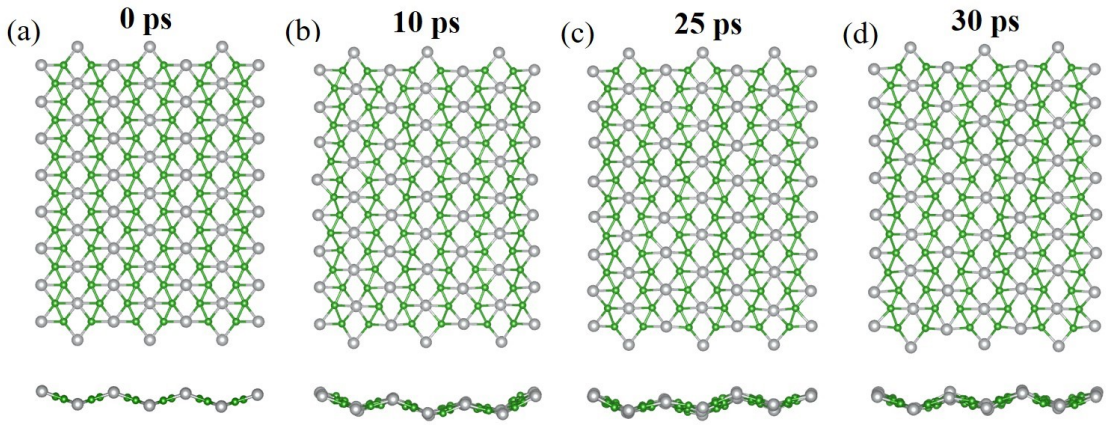

Fig. S1 (a-d) Snapshots of geometric structure for NiB_2 monolayer during AIMD simulation at 0ps, 10ps, 25ps and 30ps, respectively.

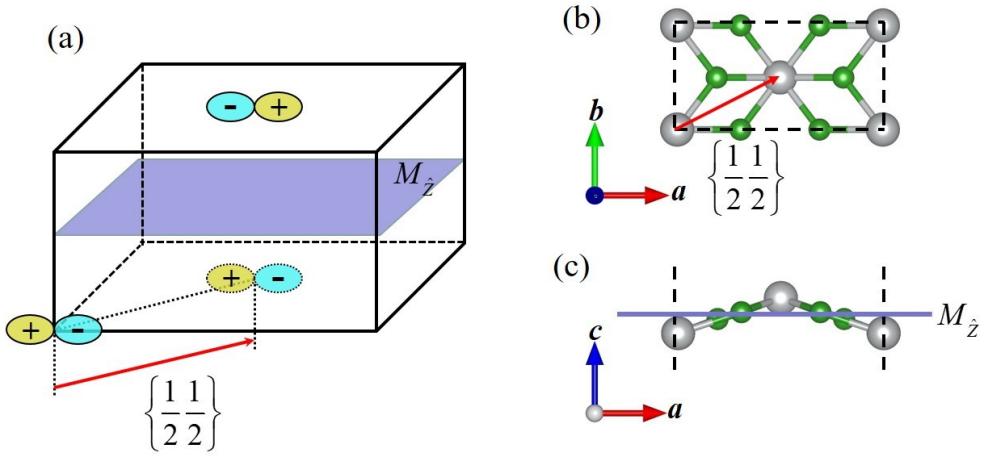

Fig. S2 (a) Schematic diagram of glide mirror symmetry in NiB_2 monolayer. The yellow and cyan parts represent the wave function whose eigenvalue under the operation of glide mirror is -*i*. (b) The corresponding operation diagram in NiB_2 monolayer.

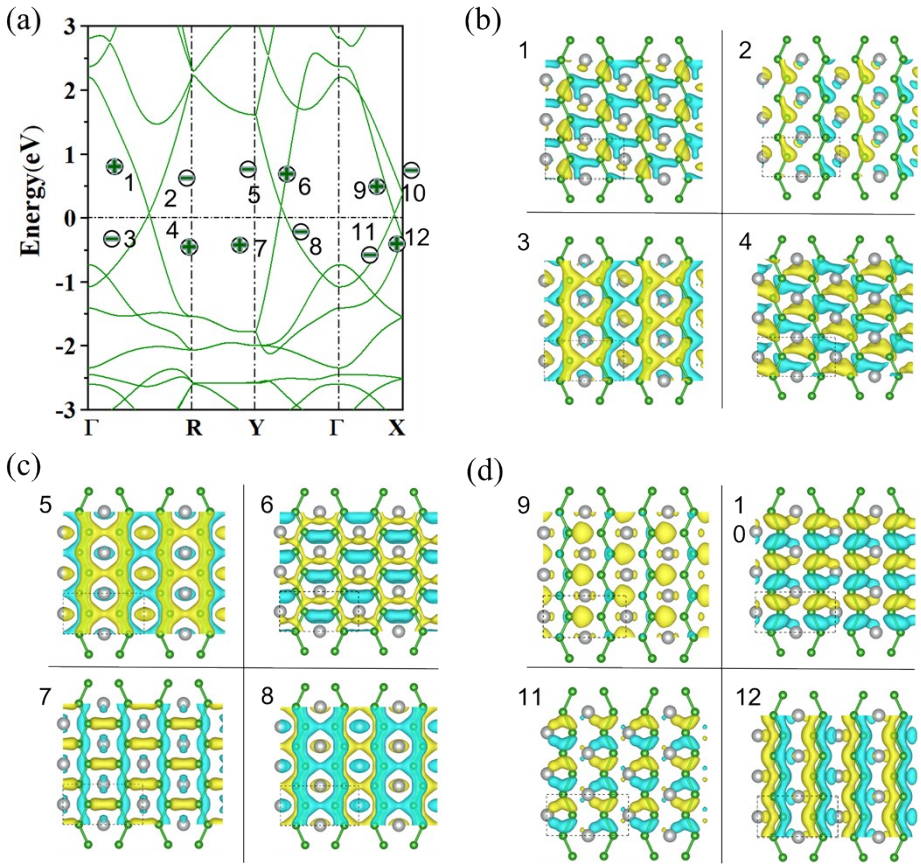

Fig. S3 (a) Calculated band structure of NiB_2 monolayer. (b-d) Real part of Kohn-Sham wave functions near band crossing points.

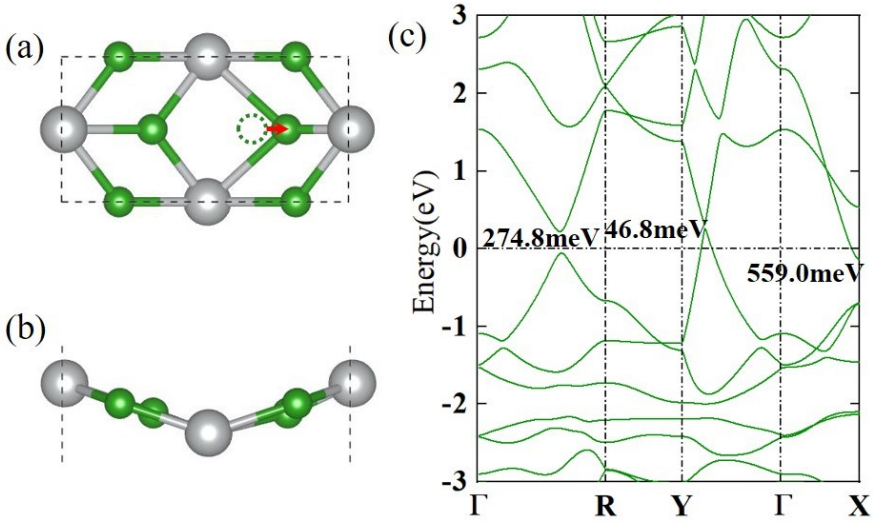

Fig. S4 (a-b) Top and side views of geometric structure for distorted NiB_2 monolayer. The green dotted line represents the equilibrium position of B atom. (c) The band structure of distorted NiB_2 monolayer.

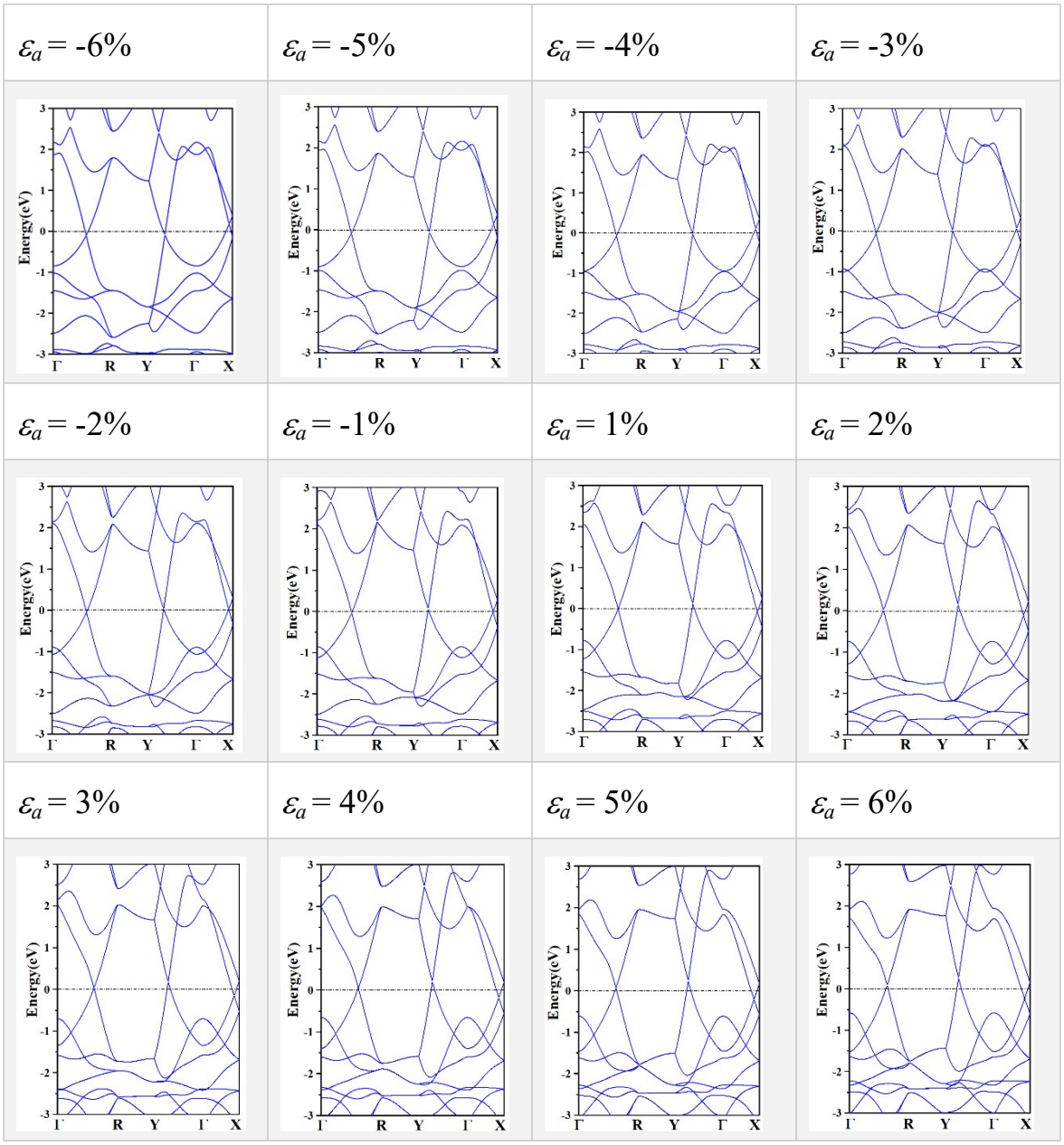

Fig. S5 Obtained band structures of NiB_2 monolayer under uniaxial strain along *a* direction.

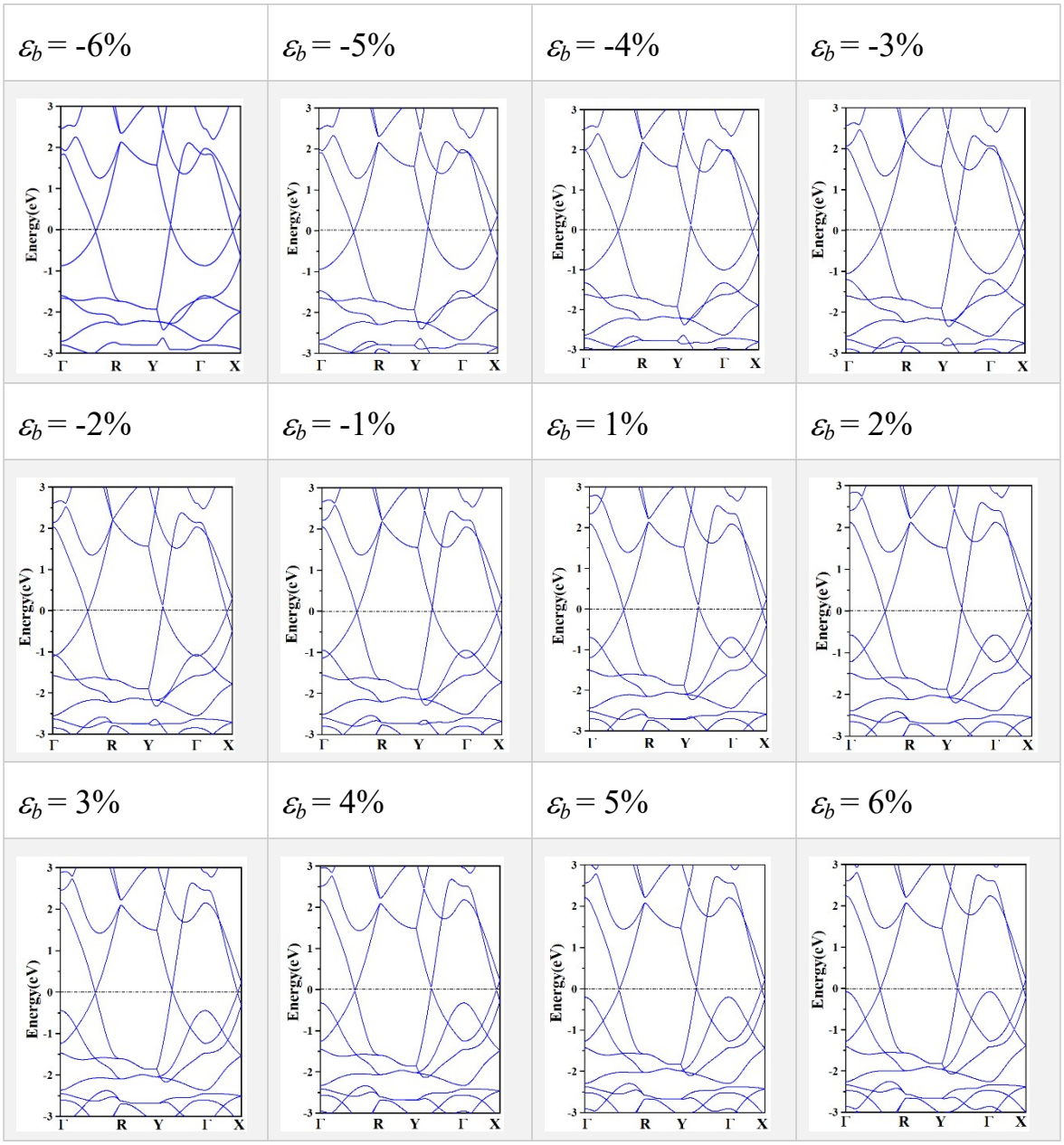

Fig. S6 Obtained band structures of NiB_2 monolayer under uniaxial strain along *b* direction.

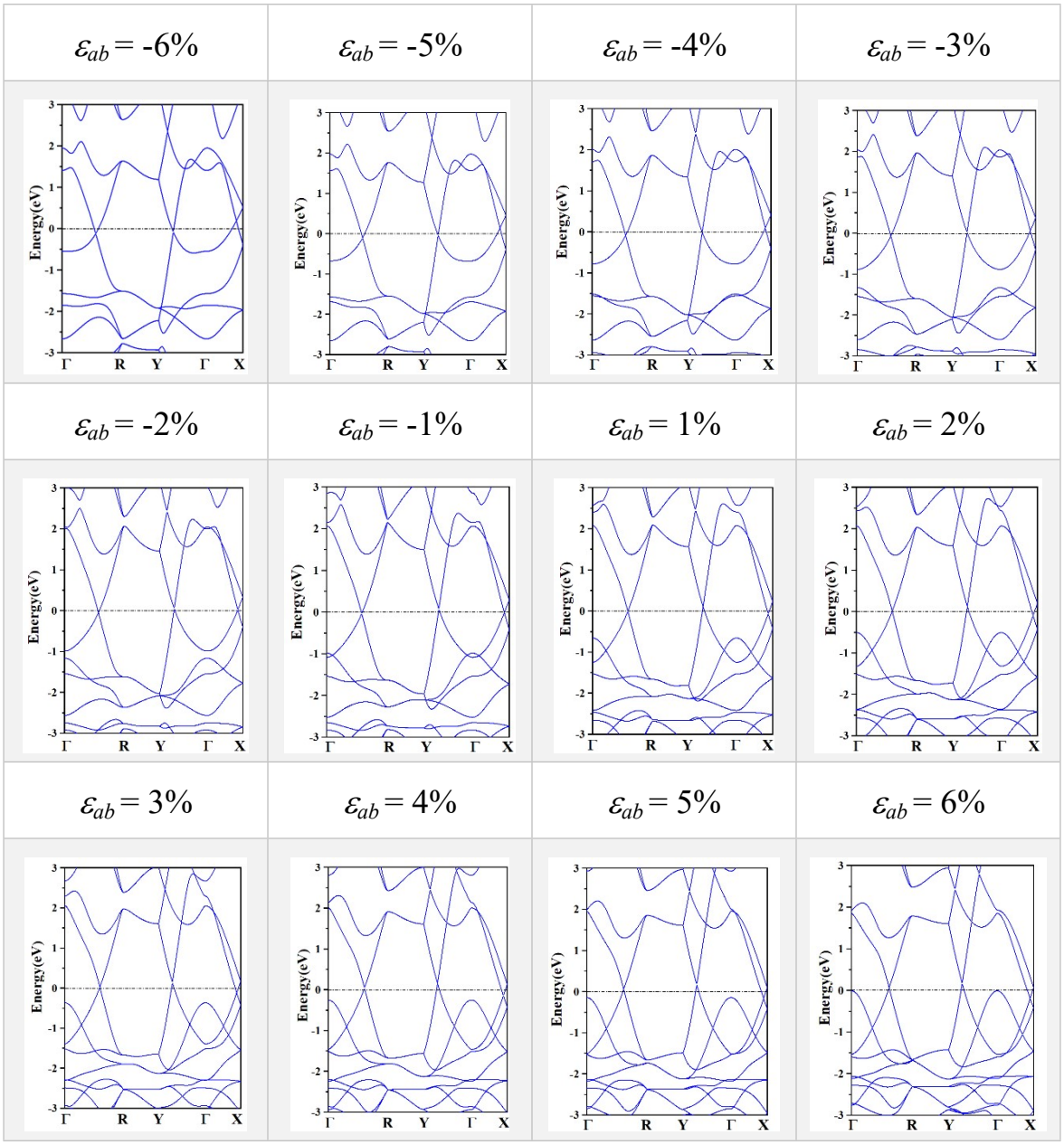

Fig. S7 Obtained band structures of NiB_2 monolayer under biaxial strain.

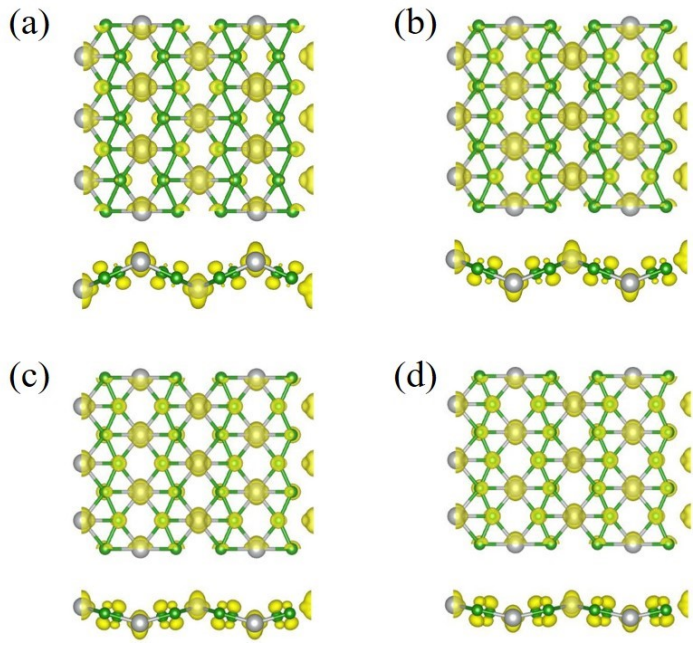

Fig. S8 The partial charge density of band crossing point P2 under different *a*-axial strain: (a) -6%, (b) -3%, (c) 3%, (d) 6%.

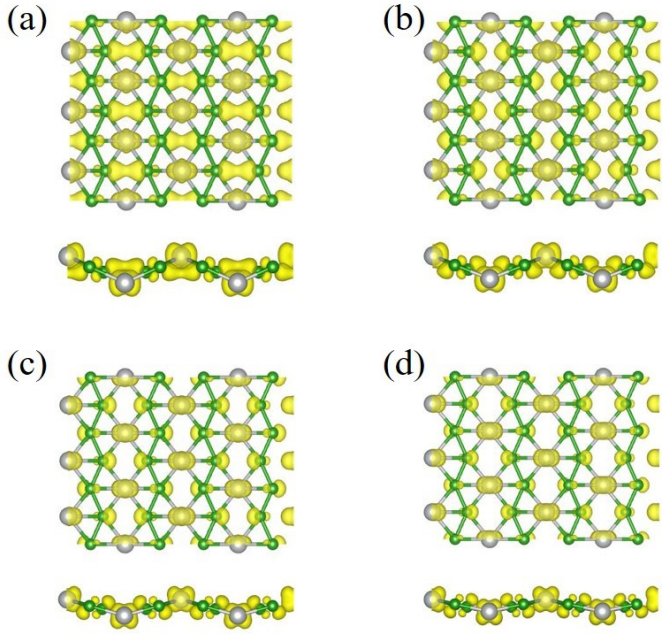

Fig. S9 The partial charge density of band crossing point P3 under different *a*-axial strain: (a) -6%, (b) -3%, (c) 3%, (d) 6%.

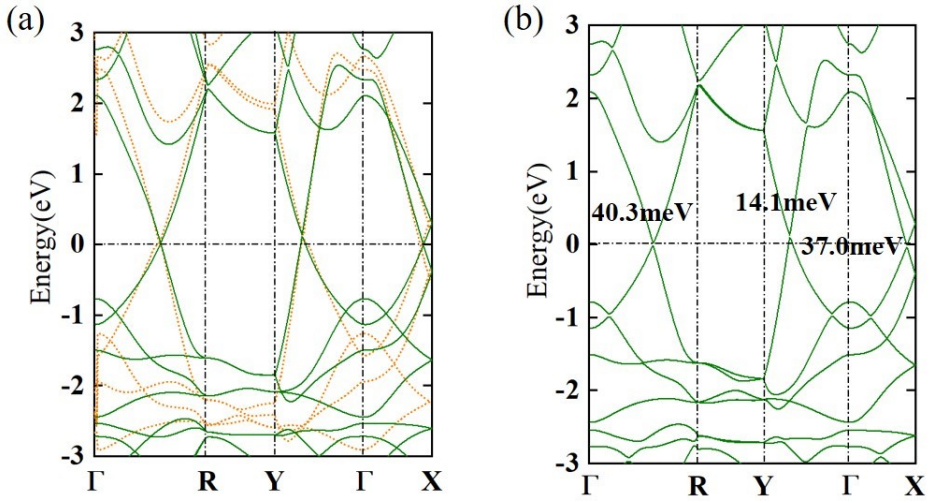

Fig. S10 (a) Calculated band structures of NiB_2 monolayer by PBE+U (green solid line, U=5.1eV) and HSE06 (yellow dotted line) functionals. (b) Calculated band structure with SOC effect.

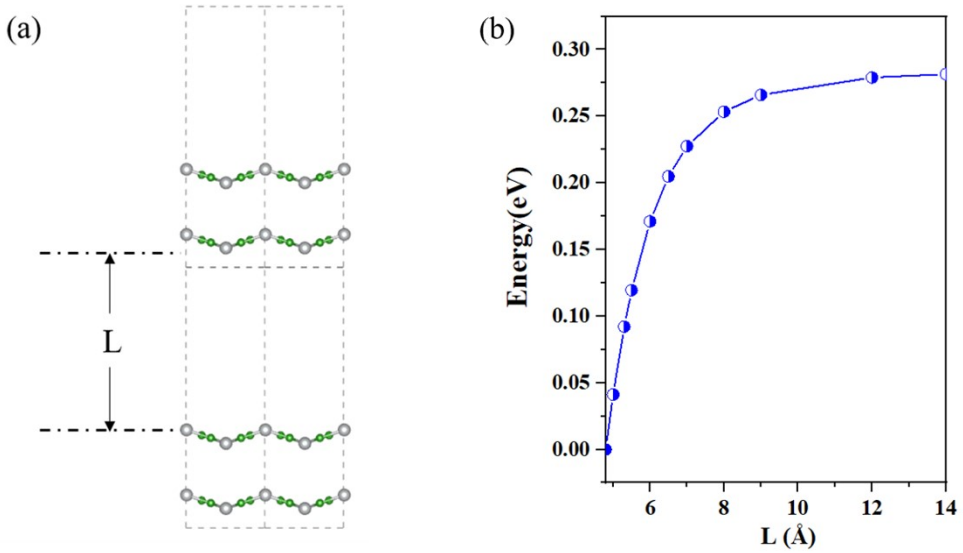

Fig. S11 (a) Schematic diagram on the calculation of exfoliation energy. (b) Calculated exfoliation energy of NiB_2 monolayer.

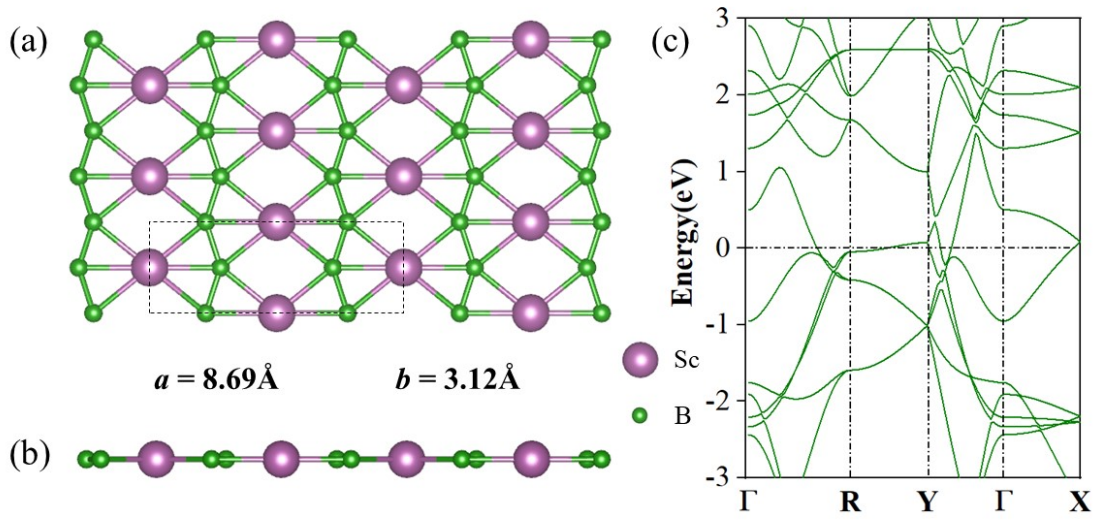

Fig. S12 (a-b) Top and side views of geometric structure for ScB_2 monolayer. (c) Calculated band structure of ScB_2 monolayer. The spin up and down channels are degenerate.

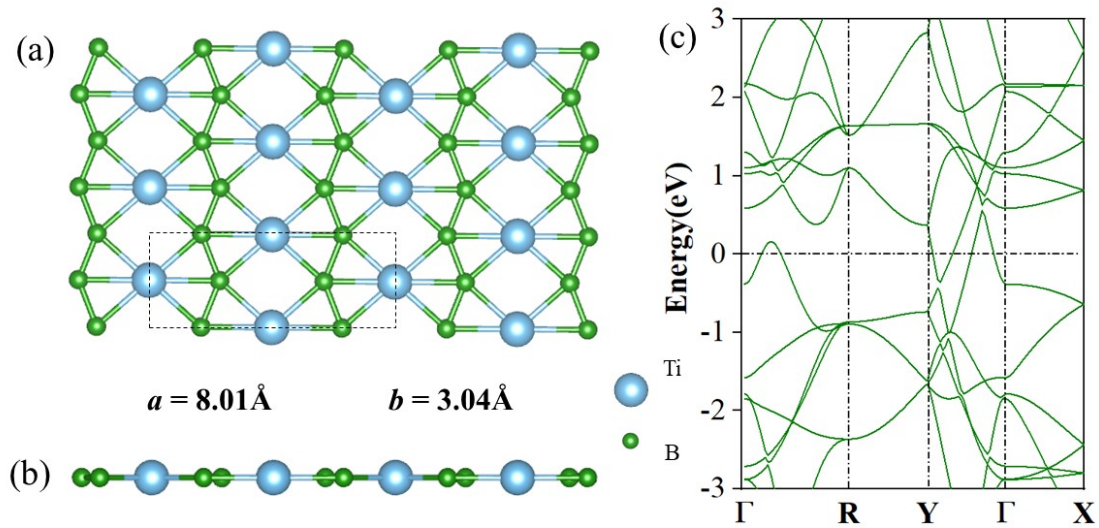

Fig. S13 (a-b) Top and side views of geometric structure for TiB_2 monolayer. (c) Calculated band structure of TiB_2 monolayer. The spin up and down channels are degenerate.

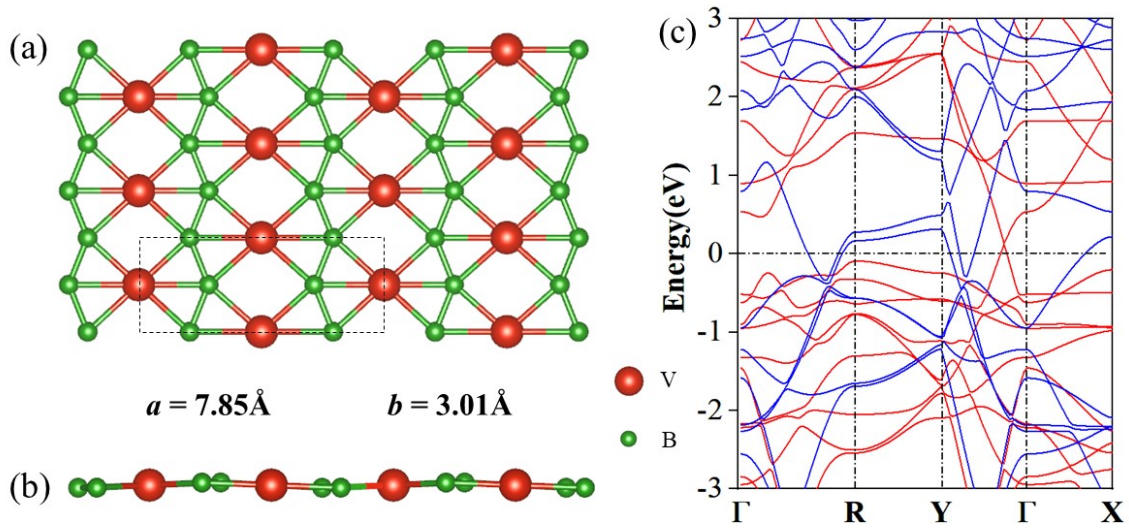

Fig. S14 (a-b) Top and side views of geometric structure for VB_2 monolayer. (c) Calculated band structure of VB_2 monolayer. The red and blue lines represent spin up and down channels, respectively.

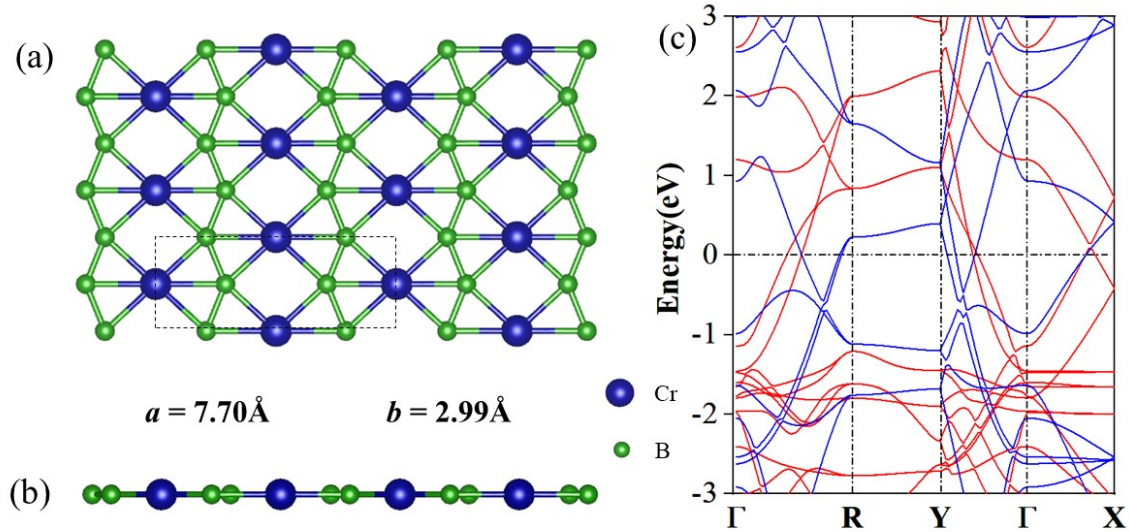

Fig. S15 (a-b) Top and side views of geometric structure for CrB_2 monolayer. (c) Calculated band structure of CrB_2 monolayer. The red and blue lines represent spin up and down channels, respectively.

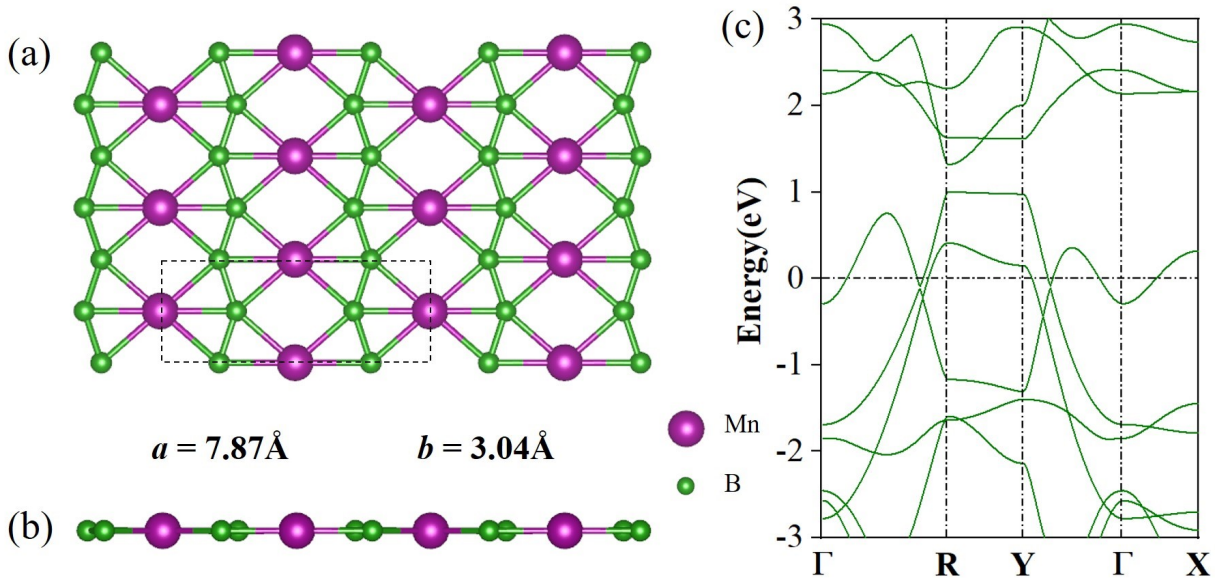

Fig. S16 (a-b) Top and side views of geometric structure for MnB_2 monolayer. (c) Calculated band structure of MnB_2 monolayer. The spin up and down channels are degenerate.

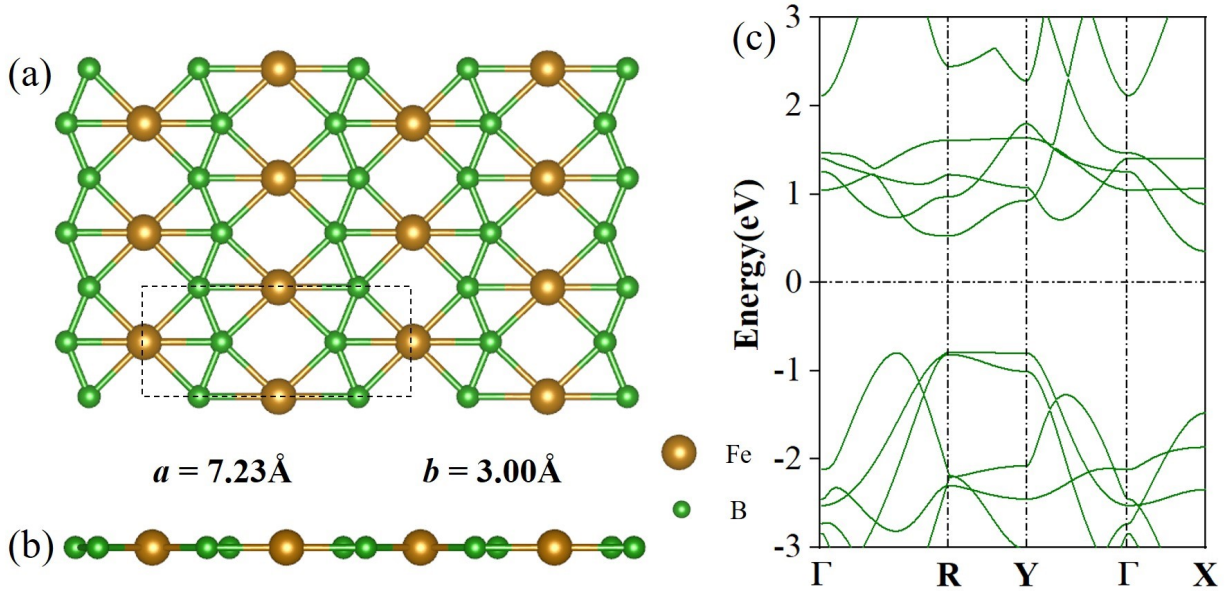

Fig. S17 (a-b) Top and side views of geometric structure for FeB_2 monolayer. (c) Calculated band structure of FeB_2 monolayer. The spin up and down channels are degenerate.

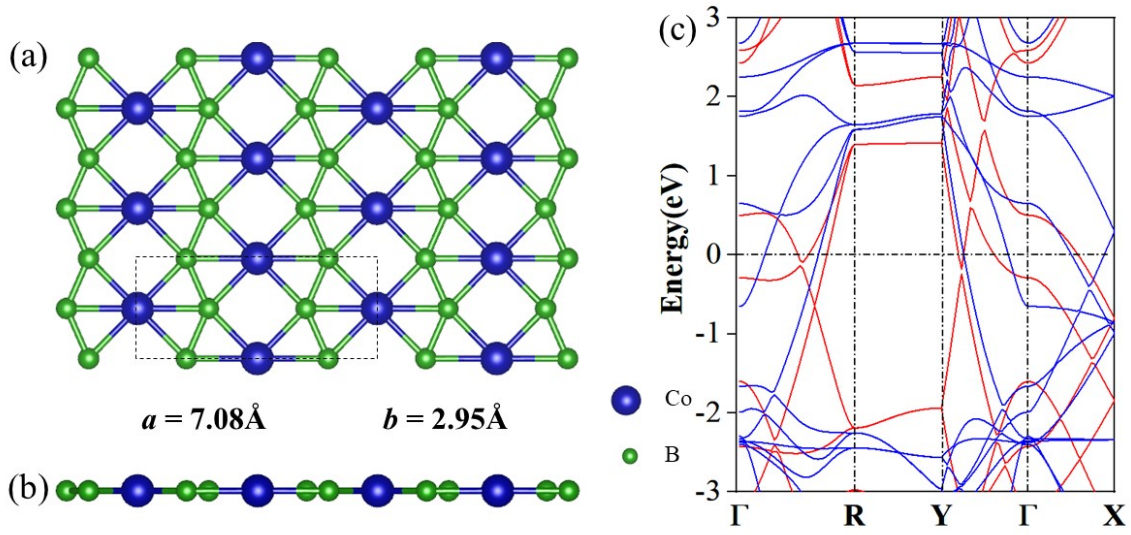

Fig. S18 (a-b) Top and side views of geometric structure for CoB_2 monolayer. (c) Calculated band structure of CoB_2 monolayer. The red and blue lines represent spin up and down channels, respectively.

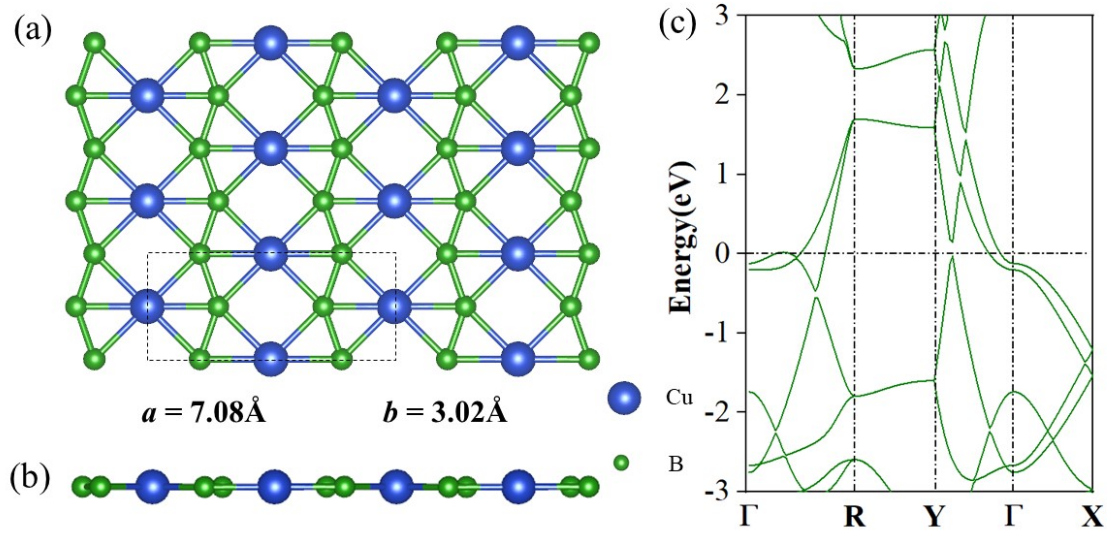

Fig. S19 (a-b) Top and side views of geometric structure for CuB_2 monolayer. (c) Calculated band structure of CuB_2 monolayer. The spin up and down channels are degenerate.

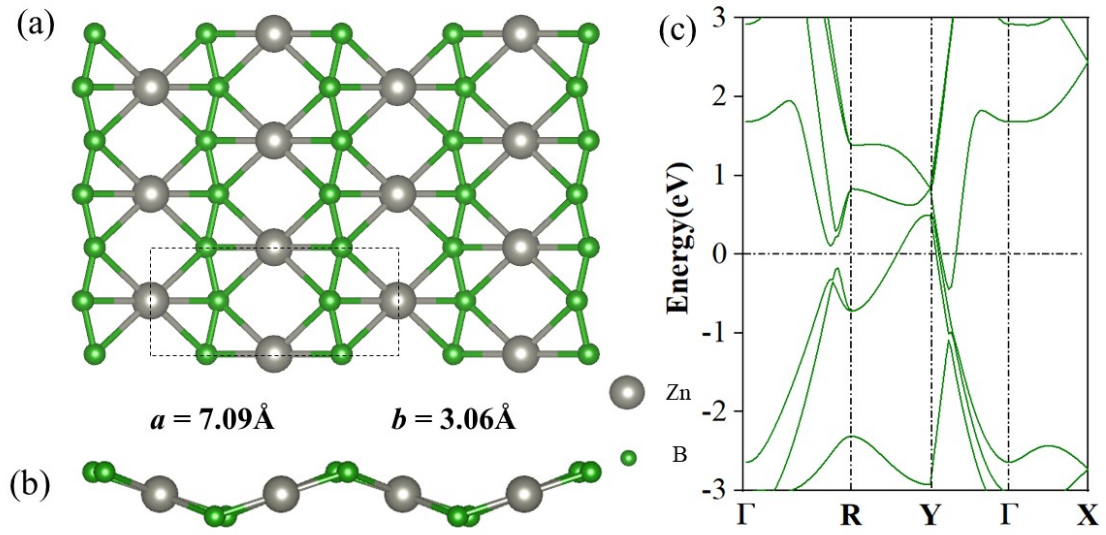

Fig. S20 (a-b) Top and side views of geometric structure for ZnB_2 monolayer. (c) Calculated band structure of ZnB_2 monolayer. The spin up and down channels are degenerate.